

Material Science and Engineering with Advanced Research

Structure and Properties Evolutions for Hard Magnetic MnAl and MnGa Based Alloys Prepared by Melt Spinning or Mechanical Milling

Zhongwu Liu^{1*}, Kunpeng Su², Yitian Cheng¹, and Raju V Ramanujan³

¹School of Materials Science and Engineering, South China University of Technology, Guangzhou, 510640, PR China

²Institute of Materials Physics, Hangzhou Dianzi University, Hangzhou, 310018, PR China

³School of Materials Science and Engineering, Nanyang Technological University, 50 Nanyang Avenue, Singapore, 639798, Singapore

***Corresponding Author:** Prof. Zhongwu Liu, PhD (Shef), MEng (USTB), BEng (CSU), Deputy Director, Department of Metallic Materials Science and Engineering, School of Materials Science and Engineering, South China University of Technology, Guangzhou, 510640, PR China, Tel/Fax: +86-20-22236906; Email: zwliu@scut.edu.cn.

Article Type: Research, **Submission Date:** 30 March 2015, **Accepted Date:** 27 April 2015, **Published Date:** 11 May 2015.

Citation: Zhongwu Liu, Kunpeng Su, Yitian Cheng, and Raju V Ramanujan (2015) Structure and Properties Evolutions for Hard Magnetic MnAl and MnGa Based Alloys Prepared by Melt Spinning or Mechanical Milling. Mater. Sci. Eng. Adv. Res 1(1): 12-19. doi: <https://doi.org/10.24218/msear.2015.03>.

Copyright: © 2015 Prof. Zhongwu Liu. This is an open-access article distributed under the terms of the Creative Commons Attribution License, which permits unrestricted use, distribution, and reproduction in any medium, provided the original author and source are credited.

Abstract

Mn-based alloys are generally thought to be the potential rare earth free permanent magnets with acceptable magnetic properties due to its available high magnetization and anisotropy field. In this work, MnAl and MnGa based alloys have been investigated regarding to their processing, structures and magnetic properties. MnAl based alloys with various C additions and/or trace rare earth doping were prepared by melt spinning. The phase transitions during rapid quenching and post annealing were investigated. The composition and annealing process dependent magnetic properties were obtained. The anisotropic MnAlC flakes with improved magnetic properties were also fabricated by surfactant assisted ball milling using alloy ingot as the precursor. The effects of ball milling and post annealing processes on the phase structure and magnetic properties were discussed. As for Mn-Ga alloy, Mn₇₀Ga₃₀ binary alloy were prepared by melt spinning followed by post heat treatment. The preliminary results show relatively high coercivity. In addition, the prospect of MnAl and MnGa based alloys for permanent magnet applications were discussed in this paper.

Keywords: Permanent magnet; Mn-Al based alloys; Mn-Ga alloy; Melt spinning; Surfactant assisted ball milling.

Introduction

As is well known, rare earth (RE) resource has become a major concern in the international community. Developing strong permanent magnets without RE elements is urgently in need. Current interests towards RE free magnets have been aimed at Mn based compounds [1]. The fundamental behind this is that Mn atom has large atomic magnetic moment. For the alloys with only one magnetic element of Mn, the magnetic moment strongly depends on the atomic distance [2]. Currently, three types of Mn-based alloys, MnAl, MnBi and MnGa, are suggested to be good hard magnets with acceptable properties. They all have high magnetic anisotropy, typically higher than 1×10^7 erg/cc, at room temperature. For MnBi alloys, high coercivity (H_c) value (>10 kOe) can be obtained at even 150°C. MnAl compound

is characterized with relatively high saturation magnetization M_s (720 emu/cc) and relatively high Curie temperature T_C (380°C). For MnGa compound, the exchange interactions of ferrimagnetism or ferromagnetism can be modified by adjusting the Mn content, and good hard magnetic properties were also reported. Most importantly, these RE-free magnets can be produced by cost-effective and sustainable manufacturing processes [1,2].

Mn-Bi alloys have been extensively studied due to their low temperature hard magnetic phase, and their magnetic properties increase with increasing temperature in a certain range. They can be prepared by various processes including melt spinning, ball milling, etc. Excellent magnetic properties have been obtained [3]. For Mn-Al alloys, the existing results [1] show that the alloys slightly above the equi-atomic composition have superior mechanical strength, excellent machinability and reasonable magnetic properties. Their theoretical maximum energy product $(BH)_{max}$, magnetocrystalline anisotropy field H_A and M_s are reported to be 101 kJ/m³, 3024 kA/m and 0.96 T, respectively [4]. Its hard magnetic properties derived from the formation of a L1₀ intermetallic phase (tetragonal τ -MnAl) with strong uniaxial magnetocrystalline anisotropy [5-7]. Unfortunately, the L1₀ (or τ) phase is a metastable one forming from a quenched-in high-temperature antiferromagnetic hexagonal disordered ϵ -phase (Neel temperature $T_N = 97$ K) by annealing at $\sim 550^\circ\text{C}$ [8]. The addition of a small amount of carbon was found to stabilize the τ phase and prevents the decomposition of the alloy into the stable but nonmagnetic γ (Al₈Mn₅) and β (Mn) phases. Some investigations showed that the alloy with 1.7 at.% C have the best hard magnetic properties since the uniformly dispersed fine Mn₃AlC phases in τ phases can pin the domain wall and improve the coercivity [4,9-11]. The best magnetic properties with $(BH)_{max}$ up to 64.4 kJ/m³ were reported in an anisotropic Mn-Al-C alloy obtained by high-temperature extrusion [12,13]. Despite above progress, MnAl-based alloys have not been fully studied and explored, possibly due to the existing of the RE magnets with extremely high magnetic properties. There are not many publications on Mn-Al alloys since early this century except some work on Mn-Al thin films [14,15]. In particular, except the work

by Fazakas *et al.* [16] and our recent work [17], synthesis of MnAl based hard magnetic alloys by rapid quenching has received almost no attention. The MnAl magnets with elemental addition other than C have also seldom been reported. In addition, up to now, MnAl-based hard magnetic alloys have not been prepared by surfactant-assisted ball milling (SABM) technique yet. As is well known, SABM has drawn great attention recently for the fabrication of high performance anisotropic NdFeB [18,19] and SmCo [20-22] hard magnetic nanoparticles and sub-micro-flakes with controlled particles size and shape.

Another Mn based alloy, Mn-Ga, has also been reported to possess large H_C value due to the formation of ferromagnetic MnGa phase or ferromagnetic Mn_3Ga phase [23]. Recent work [12,22] has shown very good properties in Mn-Ga thin films, but preparations of bulk Mn-Ga alloys or Mn-Ga powders with expected hard magnetic properties have not been very successful [24]. Investigations of Mn-Ga alloys fabricated by conventional methods like melt spinning or ball milling are, therefore, of significance.

In this paper, we report the composition and process dependent properties of MnAl(C,RE) alloys prepared by melt spinning. Both heavy RE element Dy and light RE element Pr were employed to investigate the effect of RE on the magnetism of Mn based alloy. The phase transformations and the effect of heat treatment on MnAlC alloys prepared by SABM were also investigated. The formation mechanism of submicron flakes has been discussed. In addition, the preliminary work on $Mn_{70}Ga_{30}$ alloy prepared by melt spinning are described here.

Experimental

Both melt spinning and ball milling processes were employed to achieve expected structure and properties in MnAl based alloys. For melt spun alloys, Mn-Al ingots with various nominal compositions, including $Mn_{55-x}Al_{45}C_x$ and $Mn_{52.3}Al_{45}C_{1.7}RE_1$ (RE=Pr or Dy) were prepared by argon arc melting. Pr and Dy were chosen as the doping RE elements since they represent the typical light and heavy RE element, respectively, and may give various magnetism. Special care has been paid to melting the alloys due to the big differences in the melting point and saturated vapor pressure for the raw materials of Mn, Al and C. The as-cast ingots were used to fabricate ribbon samples by a single-roller melt spinning technique under argon atmosphere at a wheel speed of 40 m/s. Selected ribbons were annealed at 500~650°C for 10 min. For the surfactant assisted ball milling (SABM) process, argon melt $Mn_{51}Al_{46}C_3$ (at.%) ingots were annealed at 1150°C for 16h followed by water quenching to form the ϵ -phase. The ingots were then manually crushed and ground down to small size less than 400 μ m. High-energy ball milling of crushed ingot was carried out for different milling time in a hardened stainless steel vial using a QM-3SP2 ball mill. Oleyl amine and Heptane (99.8%) was used as the ball-milling medium. The oleic acid (OA) (90%) was used as the surfactant with the concentration of 20.wt% of the starting powders. The ball-to-powder weight ratio was about 20:1. After ball milling, the slurry in the solution was collected and dried for further material characterization. The as-milled powders were annealed at temperatures from 400 to 650°C for 30 min to produce the ferromagnetic $L1_0$ τ -phase. Some quenched bulk samples (ingot) were also annealed under the same conditions for comparison. For Mn-Ga alloy, the ingots with designed composition were similarly prepared by argon melt and melt spinning with a wheel speed of 50 m/s. Again, it

remains a challenge to arc melt the alloys consisting of Mn and low melting point element Ga. As spun ribbons were heat treated at 673~1073K for 1 h.

The phase structure of the samples was examined by X-ray diffraction (Philips, Cu $K\alpha$ radiation). Differential scanning calorimeter (Perkin-Elmer TGA7) was employed to study the structural transformations in selected temperature range with temperature increase rate of 20°C/min. The magnetic properties at various temperatures were characterized by a PPMS (Quantam Design Co.) equipped with a VSM using an applied field of 5 T. The alloys composition was characterized by X-ray energy disperse spectrum (EDS). The microstructure was characterized by scanning electronic microscopy (SEM).

Results and Discussion

MnAl based alloys produced by melt spinning

Mn-Al(-C) and Mn-Al-C-Pr/Dy alloys with selected compositions were prepared by melt spinning. The final compositions of the ribbons have been confirmed very close to the nominal compositions based on the statistical Energy-dispersive X-ray spectroscopy (EDS) analysis on selected samples [17]. The XRD patterns for as-spun ribbons are shown in Figure 1.

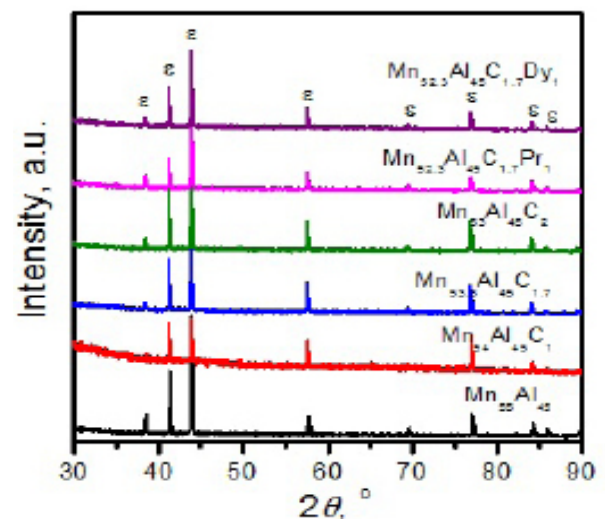


Figure 1: XRD patterns for as-spun MnAl based alloys with various compositions

All alloys have a single phase structure consisting of pure ϵ phase. The C, Pr and Dy additions have no significant effect on the phase structure.

DSC analysis was carried out to investigate the phase transition temperatures. As shown in Figure 2.

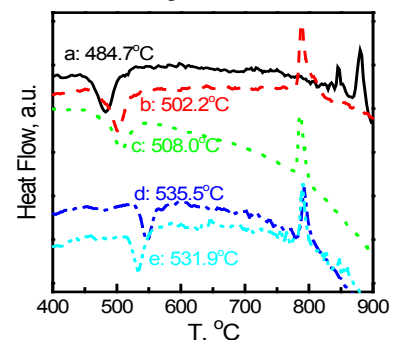


Figure 2: DSC curves for melt spun alloys: (a) $Mn_{55}Al_{45}$ (b) $Mn_{54}Al_{45}C$ (c) $Mn_{53.3}Al_{45}C_{1.7}$ (d) $Mn_{52.3}Al_{45}C_{1.7}Pr$ (e) $Mn_{52.3}Al_{45}C_{1.7}Dy$

All compositions exhibit at least two phase transitions on heating from room temperature to 900°C. For Mn₅₅Al₄₅ alloy, the sharp exothermic peak at 484.7°C corresponds to the structural transformation of the quenched-in ε-phase to the metastable magnetic τ-phase. The endothermic peak around 850°C corresponds to the transformation of the τ-phase back into the non-magnetic ε-phase. The endothermic peak around 875°C indicates the precipitations of β phase and γ phase [17]. For C added alloys, only two peaks appeared. The first peak at 500~550°C and the second peak around 800°C correspond to ε→τ and τ→ε transformations, respectively, as above. 1% C addition reduces the τ→ε transformation temperature from ~850 to < 800°C. C and RE additions change the ε→τ transformation temperature but have no significant effect on the τ→ε transition. C slightly increases the ε→τ transformation temperature and Pr or Dy also pushes this transformation to higher temperature. The results indicate that C can stabilize the τ-phase and prevent it decomposition into nano-magnetic phases.

Based on DSC results, all samples were annealed at 500~650°C to obtain hard magnetic τ phase. L1₀ phase has been formed for all alloys with C doping at the temperatures higher than 500°C. The XRD patterns for Mn₅₅Al₄₅ annealed at 550 and 600°C and for other compositions annealed at 600°C are shown in Figure 3.

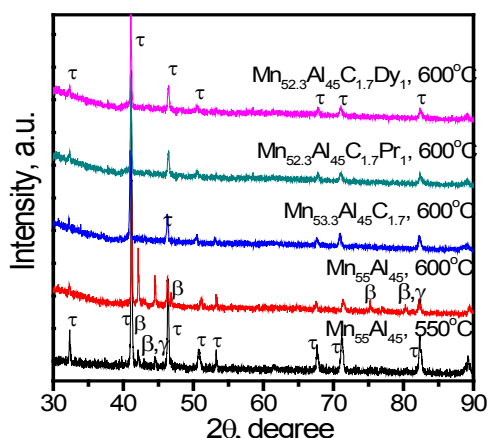


Figure 3: XRD patterns for the alloys annealed at 600 °C or 550°C

The binary Mn-Al alloy consists of mixed γ, β and τ phases. With increasing temperature from 550°C to 600°C, the contents of γ and β phases increase at the expense of τ phase. The results clearly show that τ phase decomposed into the stable γ and β phases in the binary alloy. A small amount of C addition indeed stabilizes the hexagonal metastable L1₀ phases and prevents the ε phase's decomposition into γ and β phases [6,17]. Also, co-doping Pr or Dy with C did not change the phase structure of heat treated Mn-Al-C alloys.

The magnetic properties of Mn-Al-C alloys annealed at various temperatures are shown in Figure 4.

The binary Mn₅₅Al₄₅ alloy has relatively low magnetic properties due to the mixed phase structure of τ, β, and γ phases. C ad-

dition improves the hard magnetic properties since it promotes the precipitation of τ phase and also stabilizes the τ phase, as discussed as above. High H_A of τ phase increases the coercivity of the sample. It is indeed found that the MnAlC alloy with 1.7 at.% C has the best combined magnetic properties.

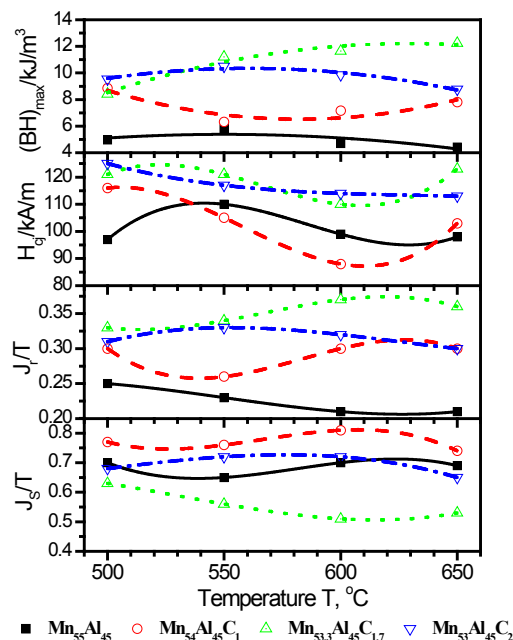


Figure 4: Magnetic properties for MnAl(C) alloys with various C contents annealed at various temperatures

$J_s=0.83$ T, $J_r=0.30$ T, $H_{cj}=123$ kA/m, and $(BH)_{max}=12.24$ kJ/m³ were obtained in the alloys annealed at 650°C. This is in good agreement with previous studies [10,12]. The J_r and $(BH)_{max}$ slightly increase with the increasing annealing temperature, possibly due to the improved transformation of hard magnetic phase. High coercivity for the alloy with 1.7 at.% C may also result from, as pointed out by Ohtani *et al.* [10] and Pareti *et al.* [13], the precipitation of a small amount of Mn₃AlC phases inside τ phase, which can pin the domain wall. For the alloys with 2 at.% C, the magnetic properties decrease when the annealing temperature is higher than 550°C. The reason has been attributed to the fact that too much carbon is not beneficial to the nucleation and growth of τ phase [16,17].

Table 1 shows the values of Curie temperature T_c , determined from the inflection points of M~T curves, for MnAlC alloys with various C contents after annealing at optimized temperatures. It is found that T_c is very sensitive to the C concentration. A linear decrease of T_c with C concentration is demonstrated. Introducing 1, 1.7, and 2 at.% C to Mn₅₅Al₄₅ alloy reduce the T_c from 346 to 292, 268 and 258°C, respectively. This large drop of T_c caused by C doping possibly explains the large discrepancy between the previous results obtained by Zeng *et al.* [11] and Fazakas *et al.* [16] Inevitable carbon loss likely occurred in Zeng's samples. Table 1 also shows the T_c of τ phase for MnAlC alloys

Table 1: The Curie temperature T_c for MnAl based alloys

| Alloy | Mn ₅₅ Al ₄₅ | Mn ₅₄ Al ₄₅ C ₁ | Mn _{53.3} Al ₄₅ C _{1.7} | Mn ₅₃ Al ₄₅ C ₂ | Mn _{52.3} Al ₄₅ C _{1.7} Pr ₁ | Mn _{52.3} Al ₄₅ C _{1.7} Dy ₁ |
|------------|-----------------------------------|--|--|--|--|--|
| T_c , °C | 346 | 292 | 268 | 258 | 264 | 267 |

Note: the estimated error is ±1 °C.

with 1.7 at.% C and 1% RE additions. T_c slightly decreases from 268 to 264 or 267°C for Pr or Dy additions, respectively.

Figure 5 shows the demagnetization curves at 5K for C and/or RE doped alloys after optimized annealing. It clearly shows the differences in J_s , J_r and J_{Hc} for all alloys. C addition improves the hard magnetic properties of the binary alloys by promoting the formation of hard phase. Addition of Pr can slightly improve the J_s , J_r and $(BH)_{max}$, but the effect of Dy on magnetization is not positive and it only slightly enhances the coercivity. The effects of RE on the MnAlC are possibly related to the magnetic moment of RE atoms and the exchange interaction between the Mn and RE atoms. Pr and Dy doping can enhance the anisotropy and increase the atomic distance between Mn atoms [25]. The best properties were obtained in C and Pr co-doped MnAl alloy.

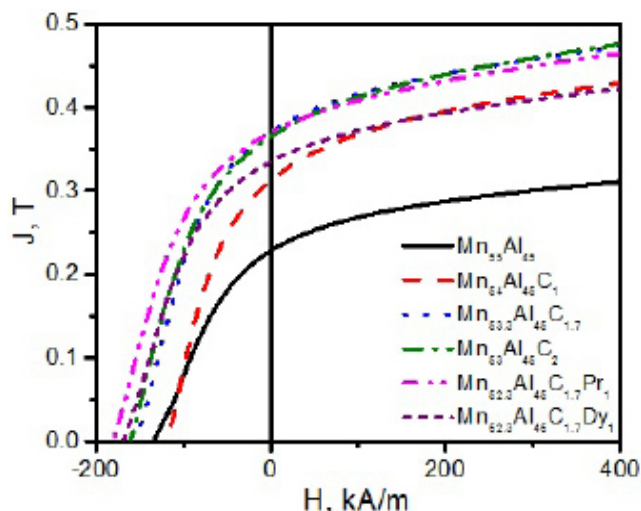


Figure 5: Demagnetization curves at 5K for optimally heat treated alloys

MnAlC flakes prepared by surfactant assisted ball milling (SABM)

SABM has been newly developed for preparing hard magnetic anisotropic NdFeB and SmCo powders [18,20]. This method has been employed for MnAlC powders in this work. XRD patterns of the $Mn_{51}Al_{46}C_3$ ingot and SABMed powders in Figure 6 indicate pure ϵ -phase. The broadened peaks for SABMed powders indicate nanocrystalline structures. The powders also show a strong (001) crystal texture. With increasing milling time from 1 to 4 hours, an increasing structural anisotropy is evident. After milling for longer time, the intensity of XRD peaks decreases gradually, resulting from the partial amorphization of the powders.

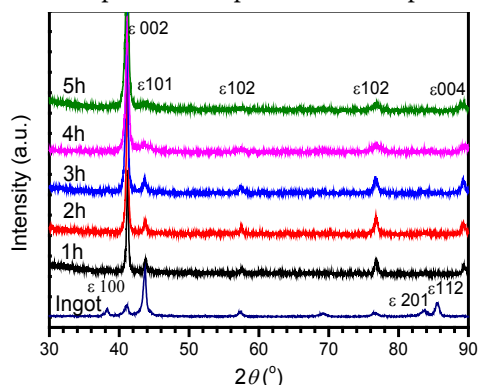


Figure 6: XRD patterns of $Mn_{51}Al_{46}C_3$ for bulk and as-milled powders
Figure 7 show the XRD patterns for $Mn_{51}Al_{46}C_3$ powders after

12 h milling and annealing at various temperatures for 30 min. Different from $Mn_{54}Al_{46}$ alloy [26,27] annealing the as-milled $Mn_{51}Al_{46}C_3$ caused the ϵ -phase to completely transform into τ -phase, even for the milling time up to 12 h. It is confirmed again that C stabilizes the ϵ -phase. Annealing at 400~500°C transforms ϵ phase into τ -phase completely. However, elevating the annealing temperature to 550°C resulted in a decomposition of τ -phase into the non-magnetic $\beta+\gamma_2$ phases. The decomposition becomes more serious with increasing temperature to 650°C.

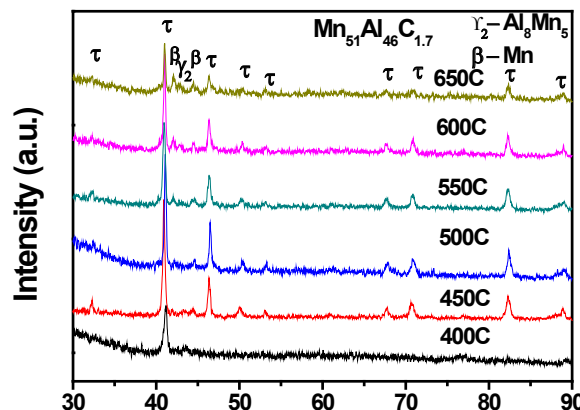


Figure 7: XRD patterns of $Mn_{51}Al_{46}C_3$ powders annealed at 400~650°C for 30 min

Figure 8 shows the SEM images of as-milled and annealed $Mn_{51}Al_{46}C_3$ flakes. High-aspect ratios are obtained in the flakes after milling for different time. From the structural examination, crushed MnAlC ingots were mainly composed of micron-sized particles 1-400 μ m in size. After milling for up to 1 h, the powders were mainly composed of micron-sized MnAlC flakes with a thickness of 10 μ m and a length of 20-150 μ m. After 4 h milling the powders were mainly composed of submicron-sized flakes with thickness of 280-840nm and length of 1-110 μ m. With increasing milling time from 4 to 8h the thickness and average length of the nanoflakes decreased significantly. The average thickness and length of the $Mn_{51}Al_{46}C_3$ flakes decreased to 132nm and 54 μ m for 8 h milling, respectively. In addition, no obvious changes were detected from the average thickness and length of the flakes before and after annealing.

The formation of MnAlC micron/submicron flakes and their subsequent transformation to texture nanoflakes during the SABM is similar to that for NdFeB [18] or SmCo [21]. In brief, the structure evolution and texture formation for the MnAlC flakes consist of the following steps: First, the internal strain in the particles increased rapidly at the beginning of ball milling, and the starting powders break into tens of microns or micron sized irregular particles. Secondly, the micro- sized particles cleaved along the easy glide basal planes to form submicron flakes. Thirdly, continuation of the cleavage of the easy glide planes via layer by layer peeling or plane splitting leads to the formation of the texture flakes. The surfactant plays multiple roles in the milling process, including preventing cold welding of crushed particles, keeping dispersion of nanoparticles, and reducing contamination during milling. Surfactant covering a particle or flake can also lower the energies of freshly claved surfaces, enable long-range capillary forces and lower the energy required for crack propagation [28,29].

The demagnetization curves for SABMed MnAlC powders annealed at 500°C are shown in Figure 9.

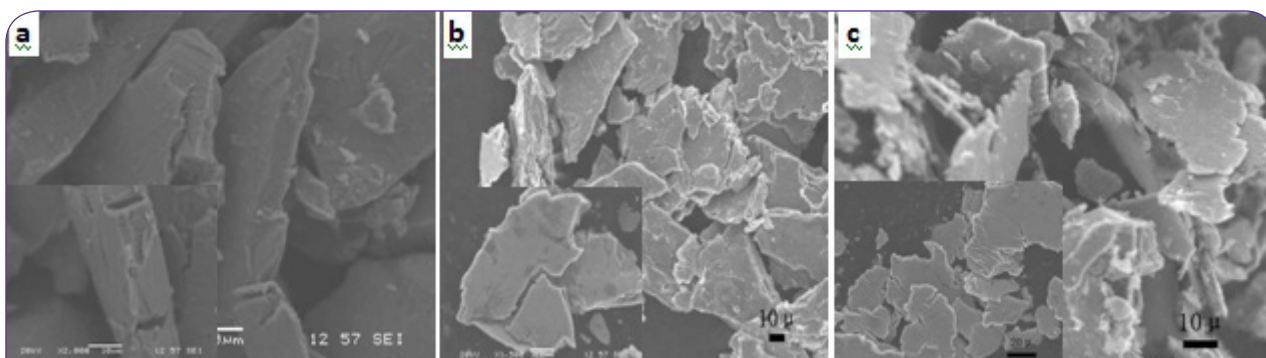


Figure 8: SEM images of the annealed Mn₅₁Al₄₆C₃ flakes obtained by ball milling for different time: a. 1 h; b. 4h; c. 8h. Insets show the flakes before annealing

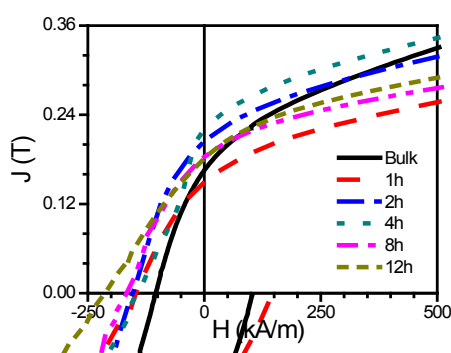


Figure 9: Hysteresis loops for bulk and SABMed Mn₅₁Al₄₆C₃ powders annealed at 500°C for 30 min

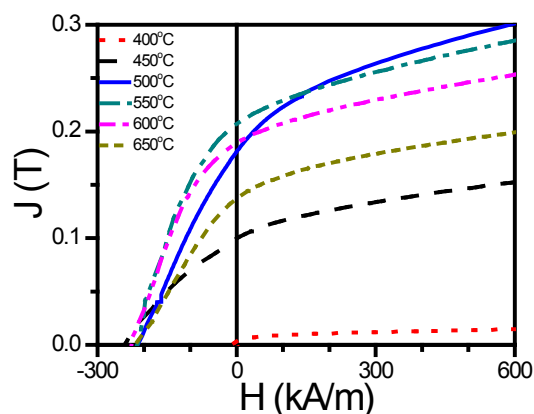


Figure 10: Demagnetization curves of SABM Mn₅₁Al₄₆C₃ powders annealed at various temperatures

The coercivity and remanence ratio J_r/J_s of bulk materials without ball milling are 106 kA/m and 0.26, respectively. Whereas for the powders subjected to ball milling, the coercivity has been enhanced. In addition, J_r/J_s has also been enhanced by ball milling. For example, the coercivity increased from 106 kA/m for the as-cast bulk sample to 148 kA/m for 1h milling. Between 1~4 hours milling, the coercivity did not change much, but it abruptly increased from 168 to 214 kA/m with further milling from 8 to 12 h. The variation in coercivity may be explained by the dependence of H_c on the τ -phase microstructure and the particle size reduction [12,29]. For those with milling periods of 1–12 h, higher H_c value originates from MnAlC powders with the fct structure. The enhancement of J_r/J_s may be contributed from the exchange-coupling interaction between the nanoscale hard grains [29]. In general, the M_s obtained in annealed SABMed samples was lower than that obtained in bulk samples. It is worth to notice that the highest M_s of 0.66 T was obtained in MnAlC ingots. The magnetization is about 68.8% of the theoretical value of 0.96T.

Figure 10 shows the demagnetization curves of SABM-milled Mn₅₁Al₄₆C₃ powders annealed at various temperatures for 30 min.

The J_s increases with the increasing annealing temperature from 400 to 500°C, and it decreases when the temperature are above 500°C. This is consistent with the XRD data that the magnetic τ phase decomposed into nonmagnetic phase when the annealing temperatures above 500°C, which leads to the reduction of magnetization. The highest J_s of 0.49T was obtained in Mn₅₁Al₄₆C₃ milled for 12 h and annealed at 500°C. The H_c had no significant change with the increasing annealing temperature from 450 to 650°C. The optimal magnetic properties for SABMed samples, $H_c=225$ kA/m and $J_r=0.21$ T, were obtained for Mn₅₁Al₄₆C₃ powders annealed at 550°C.

The highest H_c of 243 kA/m was also obtained in Mn₅₁Al₄₆C₃ annealed at 450°C. These values are much higher than that for melt spun ribbons, as shown early.

MnGa alloys prepared by melt spinning

Mn-Ga system has exhibited complicated binary phase diagram, characterized by several magnetic phases: η , γ_1 , γ_2 , and τ . It has been reported that MnGa and Mn₃Ga have potential for permanent magnets. Hyh *et al* [24]. investigated the nanostructured Mn_yGa ribbons with various concentrations prepared by melt-spinning and heat treatment. their results show that the material with $y=1.2, 1.4$, and 1.6 prefers the tetragonal L1₀ structure and that with $y=1.9$ prefers the D0₂₂ structure. A M_s of 621 emu/cm³ was found in Mn_{1.2}Ga alloy. Both the L1₀- and D0₂₂-Mn_yGa samples show a high T_c well above room temperature. The observed magnetic properties of the Mn_yGa ribbons are consistent with the competing ferromagnetic coupling between Mn moments in the regular L1₀-MnGa lattice sites and antiferromagnetic coupling with excess Mn moments occupying Ga sites. In the present work, our preliminary work focused on the Mn₇₀Ga₃₀ alloys with Mn₃Ga phase. Due to the low vaporization point of metal Mn (~1900°C) and low melting pint of Ga, it is a challenge to obtain Mn-Ga alloys with pre-designed nominal compositions. By the precious process control of argon melting, we are able to target the objective composition. Table 2 shows the DES result of the compositional analysis for melt spun Mn₇₀Ga₃₀ alloy, demonstrating that the actual composition of our alloy is very close to the target composition.

Table 2: Objective and actual compositions for melt spun Mn-Ga alloy analyzed by EDS

| Element | Objective concentration (at.%) | EDS results (at.%) |
|---------|--------------------------------|--------------------|
| Mn | 70 | 69.49 |
| Ga | 30 | 30.51 |
| Total | 100 | 100 |

Figure 11 shows the surface image of as spun Mn₇₀Ga₃₀ ribbon prepared at a wheel speed of 50 m/s. As spun alloy has uniform grain size around 1µm. It indicates that Mn-Ga alloys have relatively low glass formability and it is relatively difficult to achieve nanocrystalline structure and amorphous structures, which are different from NdFeB based hard magnetic alloys [30].

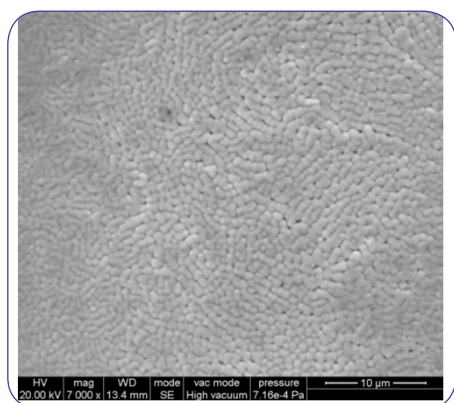


Figure 11: SEM image for the surface of as melt spun Mn₇₀Ga₃₀ ribbon

Figure 12 shows the XRD patterns for the as spun Mn-Ga alloy and the alloys after heat treatment at various temperatures. Mn₃Ga phase appears in all alloys. With increasing annealing temperature from 673 to 973K, the XRD peak intensity increases. Further increase of temperature to 1073K, the peak intensity decreases, possibly due to the start of a phase transition. The phase structure of the obtained Mn₃Ga is D0₁₉-Mn₃Ga and no D0₂₂-Mn₃Ga phase was found. It was reported that the magnetic properties of D0₁₉-Mn₃Ga phase is much lower than that of D0₂₂-Mn₃Ga phase.

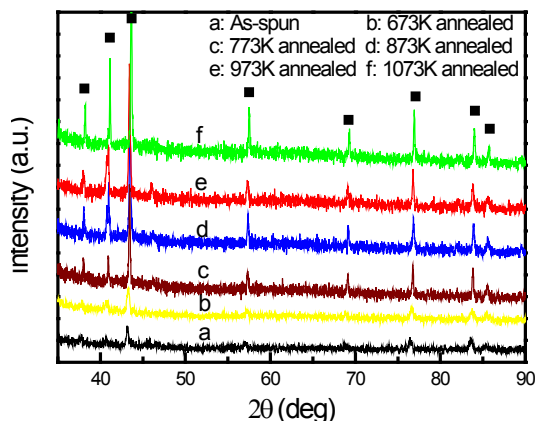


Figure 12: XRD patterns for as spun and heat treated Mn₇₀Ga₃₀

Figure 13a indicates that the as-spun MnGa has very low magnetization and coercivity.

Figure 13a shows the hysteresis loops of the as spun Mn₇₀Ga₃₀ alloy and the alloys annealed at various temperatures.

Relatively low J_s and J_r were obtained, resulting from the weak magnetism of this D0₁₉ phase. However, the J_s and H_C can be greatly improved by heat treatment. After heat treated at 873K for 1 h, the H_C of 6.72 kOe and J_r of 6.15 emu/g can be obtained. To explain the reason for the dependence of H_C on the annealing temperature, thermal analysis of DSC was carried out for the as spun Mn₇₀Ga₃₀ alloy. Figure 13b shows no DSC peak below 1000 K, indicating no first order phase transition at this temperature range. A phase transition at just above 1000 K should be responsible for the reduced magnetic properties for the alloys heat treated at 973 and 1073K. It remains a challenge to well explain the improved magnetic properties by annealing.

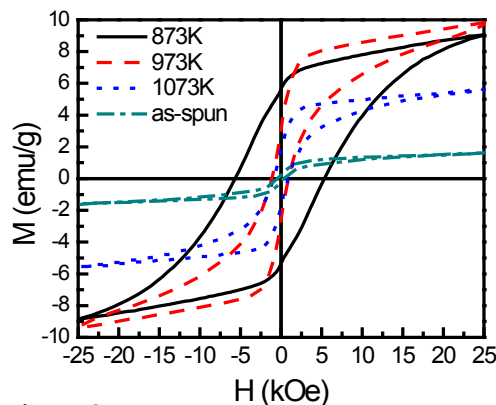


Figure 13a

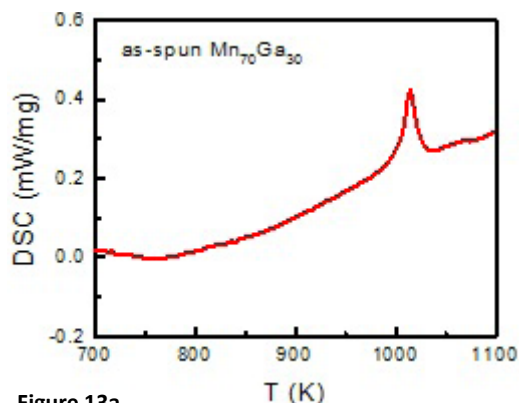


Figure 13b

Figure 13: Magnetic hysteresis for as spun Mn₇₀Ga₃₀ and Mn₇₀Ga₃₀ heat treated at various temperatures (a) and DSC curve for as spun alloy (b)

Prospects for Mn based permanent magnets

The present results showed that the magnetic properties of melt spun Mn-Al based alloys obtained so far are much lower than that reported for MnAlC magnets prepared by hot extrusion of annealed gas-atomized powders [13]. Surfactant assisted ball milling technique can enhance the magnetic properties of MnAlC alloys. Therefore, the processing has an important effect on the microstructure and properties of this type of alloys. A proper preparation and treatment process have to be developed for making full use of this low cost permanent magnet.

For MnGa based alloys, melt spinning technique has difficulty in producing nanocrystalline alloys. Since Mn₇₀Ga₃₀ alloy has relatively low glass formability, the as spun ribbons are generally micro- or submicro- crystalline. To enhance the magnetic properties, except forming the L1₀ structure in the heat treated materials, refining the grain size may be a possible approach,

which may be realized also by either doping the secondary elements or employing post-process like ball milling.

In addition, to enhance the remanence of the Mn-based alloys, magnetic anisotropy has to be pursued by advanced processes. Two processes can be proposed, i.e. magnetic field aligning the anisotropic powders and forming anisotropic crystal texture in bulk materials by deformation. To enhance the magnetism of Mn based alloys, future investigations should aim to achieve hard magnetic properties in Mn-based compounds with adjusted atomic distance by forming alloys or introducing interstitial atoms and realizing anisotropic grain structures.

Since NdFeB and hard ferrites have been well developed as the high properties high cost hard magnets and low properties low cost hard magnets, respectively, future application of Mn-based magnets should aim at low cost magnets with intermediate magnetic properties, which will fill the property gap between the NdFeB and Sr-/Ba- ferrites. To achieve this goal, extensive work have to be carried out in this field.

Conclusion

The effects of composition and heat treatment on the phase transition and magnetic properties of MnAl based alloys prepared by melt spinning have been investigated. Addition of C is beneficial to the formation of τ phase. The $Mn_{53.3}Al_{45}C_{1.7}$ ribbon after annealed at 650°C for 10 min has the best combined magnetic properties. C content also has a significant effect on the T_C of τ phase. Doping of rare earth element Pr can slightly improve the hard magnetic properties, but Dy does not have positive effect on magnetization. Anisotropic MnAlC flakes with various sizes and thicknesses were fabricated by SABM. The as prepared flakes consist only of the hcp structured ϵ -phase, which can completely transform to the metastable ferromagnetic τ -phase after annealing at a proper temperature. C addition cannot prevent the decomposition of the τ -phase into the equilibrium non-magnetic $\beta+\gamma_2$ phases at the temperature above 500°C. The magnetic properties are strongly dependent on the fraction of the τ -phase and ball milled time. A high coercivity of 242.8 kA/m and a saturation magnetization of about 0.49 T were obtained in SABMed flakes, which are much higher than that for melt spun ribbon. In addition, preliminary results on melt spun Mn-Ga alloy have been obtained. Heat treatment can significantly improve the magnetic properties of as-spun $Mn_{70}Ga_{30}$ alloy. High coercivity of 6.72 kOe has been obtained after heat treatment. The present results indicated that the properties of Mn-Al and Mn-Ga based alloys are very much dependent on the preparation method.

Acknowledgments

This work is partly supported by the program for New Century Excellent Talents in University (Grant No. NCET-11-0156) and the Scientific Research Foundation of Hangzhou Dianzi University (Grant No.KYS205612007).

References

1. Coey JMD. New permanent magnets; manganese compounds. *J Phys Condens Matter*. 2014; 26(6): 064211.
2. Skomski R, Manchanda P, Kumar P, Balamurugan B, Kashyap A, Sellmyer DJ. Predicting the future of Permanent-Magnet Materials. *IEEE Trans. Magn.* 2013; 49(7):3215-3220. doi: 10.1109/TMAG.2013.2248139.

3. Ly V, Wu X, Smillie L, Shoji T, Kato A, Manabe A, et al. Low-temperature phase MnBi compound: A potential candidate for rare-earth free permanent magnets. *J. Alloy Comp.* 2014; 615(Suppl 1): S285-S290. doi: doi:10.1016/j.jallcom.2014.01.120.
4. Chaturvedi A, Yaqub R, Baker I. A comparison of τ -MnAl particulates produced via different routes. *J. Phys.: Condens. Matter*. 2014; 26(6):064201. doi:10.1088/0953-8984/26/6/064201.
5. Kamino K, Kawaguchi T, Nagakura M. Magnetic properties of manganese-aluminum system alloys. *IEEE Trans. Magn.* 1996; 2(3):506-510. doi: 10.1109/TMAG.1966.1065887.
6. Yanar C, Wiezorek JMK, Radmilovic V, Soffa WA. Massive Transformation and the Formation of the Ferromagnetic L10 Phase in Manganese-Aluminum-Based Alloys. *Metall. Mater. Trans. A*. 2002; 33(8): 2413-2423. doi: 10.1007/s11661-002-0363-3.
7. Koch AJJ, Hokkelling P, Steeg MGVD, de Vos KJ. New material for magnets on base of Mn and Al. *J. Appl. Phys.* 1960; 31:75S -77S. doi: <http://dx.doi.org/10.1063/1.1984610>.
8. Wyslocki JJ, Pawlik P, Przybyl A. Magnetic properties of the non-oriented ϵ -phase in Mn-Al-C permanent magnet. *Mater. Chem. Phys.* 1999; 60(2):211-213. doi:10.1016/S0254-0584(99)00096-6.
9. Kono H. On the ferromagnetic phase in manganese-aluminum system. *J. Phys. Soc. Japan*. 1958; 13(12): 1444-1451. doi: <http://dx.doi.org/10.1143/JPSJ.13.1444>.
10. Ohtani T, Kato N, Kojima K, Sakamoto Y, Konno I, Tsukahara M, et al. Magnetic properties of Mn-Al-C permanent magnet alloys. *IEEE Trans. Magn.* 1977; 13:1328.
11. Zeng Q, Baker I, Cui JB, Yan ZC. Structural and magnetic properties of nanostructured Mn-Al-C magnetic materials. *J. Magn. Magn. Mater.* 2007; 308(2):214. doi:10.1016/j.jmmm.2006.05.032.
12. Yamaguchi A, Tanaka Y, Yanagimoto K, Sakaguchi I, Kato N. Development of P/M Mn-Al-C Alloy Permanent Magnet Bull. *Jpn. Inst. Met.* 1989; 28:422.
13. Pareti L, Bolzoni F, Leccabue F, Ermakov AE. Magnetic anisotropy of XnAl and 1hA1-C permanent magnetic materials. *J. Appl. Phys.* 1986; 59:3824-3828.
14. Yan ZC, Huang Y, Zhang Y, Hadjipanayis GC, Soffa W, Weller D. Magnetic and structural properties of MnAl/Ag granular thin films with L_{10} structure. *Scripta Mater.* 2005; 53(4):463-468. doi:10.1016/j.scriptamat.2005.04.045.
15. Zhu LJ, Nie SH, Zhao JH. Recent progress in perpendicularly magnetized Mn-based binary alloy films. *Chinese Phys. B*. 2013; 22(11):118505. doi:10.1088/1674-1056/22/11/118505.
16. Fazakas E, Varga LK, Mazaleyrat F. Preparation of nanocrystalline Mn-Al-C magnets by melt spinning and subsequent heat treatments. *J. Alloys Compd.* 2007; 434-435:611-613. doi:10.1016/j.jallcom.2006.08.313.
17. Liu ZW, Chen C, Zheng Z.G, Tan BH, Ramanujan RV. Phase transition and hard magnetic properties for rapidly solidified MnAl alloys doped with C, B and rare earth elements. *J. Mater. Sci.* 2012; 47(5): 2333-2338. doi: 10.1007/s10853-011-6049-8.
18. Cui BZ, Zheng LY, Li WF, Liu JF, Hadjipanayis GC. Single-crystal and textured polycrystalline $Nd_2Fe_{14}B$ flakes with a submicron or nanosize thickness. *Acta Mater.* 2012; 60(4):1721-1730. doi:10.1016/j.actamat.2011.11.062.
19. Yue M, Pan R, Liu RM, Liu WQ, Zhang DT, Zhang JX, et al. Crystallographic alignment evolution and magnetic properties of Nd-Fe-B nanoflakes prepared by surfactant- assisted ball milling. *J. Appl. Phys.* 2012; 111:07A732. doi: <http://dx.doi.org/10.1063/1.3679414>.

20. Poudyal N, Rong CB, Liu JP. Morphological and magnetic characterization of Fe, Co, and FeCo nanoplates and nanoparticles prepared by surfactants-assisted ball milling. *J. Appl. Phys.* 2011; 109:07B526. doi: <http://dx.doi.org/10.1063/1.3561157>.
21. Zheng L, Cui B, Hadjipanayis GC. Effect of different surfactants on the formation and morphology of SmCo₅ nanoflakes. *Acta Mater.* 2011; 59(17):6772-6782. doi:10.1016/j.actamat.2011.07.035.
22. Cui BZ, Li WF, Hadjipanayis GC. Formation of SmCo₅ single-crystal submicron flakes and textured polycrystalline nanoflakes. *Acta Mater.* 2011; 59(2):563-571. doi:10.1016/j.actamat.2010.09.060.
23. Zhu LJ, Zhao JH. Perpendicularly magnetized Mn_xGa films: promising materials for future spintronic devices, magnetic recording and permanent magnets. *Appl. Phys. A.* 2013; 111(2):379-387. doi: 10.1007/s00339-013-7608-4.
24. Huh Y, Kharel P, Shah VR, Li XZ, Skomski R, Sellmyer DJ. Magnetism and electron transport of Mn_yGa (1 < y < 2) nanostructures. *J. Appl. Phys.* 2013; 114:013906. doi: <http://dx.doi.org/10.1063/1.4812561>.
25. Bohlmann MA, Koo JC, Wise JH. Mn-A-C for permanent magnets. *J. Appl. Phys.* 1981; 52:2542. doi: <http://dx.doi.org/10.1063/1.328995>.
26. Wang H, Si P, Jiang W, Lee J, Choi C, Liu J, et al. Structural stabilizing effect of Zn substitution on MnAl and its magnetic properties. *Open J. Microphysics.* 2011; 1(2):19-22. doi: 10.4236/ojm.2011.12003.
27. Zeng Q, Baker I, Yan ZC. Nanostructured Mn–Al permanent magnets produced by mechanical milling. *J. Appl. Phys.* 2006; 99:08E902.
28. Gabay AM, Akdogan NG, Marinescu M, Liu JF, Hadjipanayis GC. Rare earth–cobalt hard magnetic nanoparticles and nanoflakes by high-energy milling. *J Phys Condens Matter.* 2010; 22(16):164213. doi: 10.1088/0953-8984/22/16/164213.
29. Su KP, Tao DL, Wang J, Huo DX, Cao YQ, Liu ZW, et al. Preparation of MnAlC flakes by surfactant assisted ball-milling and the effects of annealing. *Int. J. Mater. Res.* 2015; 106(1):75-79. doi: 10.3139/146.111147.
30. Liu ZW, Davies HA. Practical limits of enhancing the room temperature magnetic properties for nanocrystalline NdPrDyFeCoB alloys. *J. Magn. Magn. Mater.* 2007; 313:337-341.